

See discussions, stats, and author profiles for this publication at: <https://www.researchgate.net/publication/20738037>

Ultrastructural evidence for the presence of ferritin-iron in the biliary system of patients with iron overload

ARTICLE *in* HEPATOLOGY · JANUARY 1986

Impact Factor: 11.06 · DOI: 10.1002/hep.1840060107 · Source: PubMed

CITATIONS

16

READS

13

6 AUTHORS, INCLUDING:



[Joannes J M Marx](#)

University Medical Center Utrecht

213 PUBLICATIONS 4,777 CITATIONS

[SEE PROFILE](#)

Ultrastructural Evidence for the Presence of Ferritin-Iron in the Biliary System of Patients with Iron Overload

MAUD I. CLETON, JAN W. SINDRAM,[†] LOUK H. P. M. RADEMAKERS, FLORIS M. J. ZUYDERHOUDT,
WILLEM C. DE BRUIJN AND JOANNES J. M. MARX

Pathological Institute, University of Utrecht and Departments of Internal Medicine and Hematology, University Hospital Utrecht, Utrecht, The Netherlands; Department of Internal Medicine, Academic Medical Centre, Amsterdam, Holland; and Centre for Analytical Electron Microscopy, Laboratory for Electron Microscopy, University of Leiden, Leiden, The Netherlands

Ferritin-like particles were observed in bile canaliculi of patients with iron overload. These particles have been further investigated by: (1) a staining method enhancing the size and contrast of ferritin protein, and (2) electron probe microanalysis detecting the presence of the elements iron and phosphorus.

Morphological observation of coated vesicles in the cytoplasm adjacent to the bile canaliculi and coated pits in the canalicular membrane suggests a transport mechanism via membrane-bound organelles.

Support is given to the theory that part of the iron, stored in the liver, leaves the hepatocyte by excretion of ferritin into the bile.

Ferritin, the intracellular iron storage protein, consists of a spherical protein shell (with a molecular weight of 450,000 daltons) composed of 24 rather similar subunits, that can accommodate up to 4,500 atoms of iron (1). The particle owes its contrast in the transmission electron microscope to the electron-dense iron core of approximately 5 nm diameter. In normal hepatocytes, only very small amounts of ferritin-iron particles can be observed in cytosol and hepatic lysosomes. In hepatocytes of subjects with iron overload, however, increasing amounts of ferritin can be found dispersed through the cytoplasm, in clusters, and in lysosomal bodies, called siderosomes (2). The siderosomes are, like lysosomes, usually located around the bile canaliculi. From the work of Scheuer (3), it is known that iron deposits can be observed in the epithelial cells of the bile duct of patients with iron overload. A correlation between the amount of liver ferritin and ferritin protein in the bile of iron-loaded rats has been reported (4). Moreover, preliminary data indicate that ferritin concentrations in human bile are in the same range as in the blood (Zuyderhoudt, F. M. J., unpublished results). The combination of morphological observations and biochemical data suggests an involvement of the biliary system in iron metabolism.

In the present study, we collected ultrastructural evi-

dence for ferritin localization in the bile canaliculi of patients with iron overload.

MATERIALS AND METHODS

Liver biopsies from four patients in different stages of hemosiderosis were prepared for light and electron microscopy. In two subjects, biopsies were performed before and after phlebotomy. For light microscopy, the Perls's Prussian blue method for staining of iron was used as was the Gordon and Sweets method for reticulin. Iron deposition was graded according to Scheuer et al. (5). Serum ferritin was evaluated with the Ferritin Radioimmunoassay Kit obtained from the Radiochemical Centre, (Amersham, United Kingdom) (6). Some values of the test subjects are summarized in Table 1.

For electron microscopy, small tissue blocks were immersed immediately in a fixative containing 2.5% glutaraldehyde and 2% paraformaldehyde in 0.08 M cacodylate buffer plus 0.025% CaCl₂ (pH 7.2) for 2 hr at 4°C. As a second fixative, OsO₄ (1%) in the same buffer was used for 2 hr at 4°C. The tissue was dehydrated and embedded in Epon 812 according to standard procedures. Ultrathin (70 nm) sections left unstained or stained with uranyl magnesium acetate and lead nitrate or with bismuth subnitrate (7) were collected on pioloform-filmed 100 mesh copper grids and viewed in a Philips EM 201c.

Three biopsy specimens were selected to be studied by electron probe microanalysis. In this case, fixation in osmium was omitted, and ultrathin (70 nm) sections were collected on pioloform-filmed 100 mesh gold or tungsten grids. Analysis was performed in a Philips EM 400 analytical microscope operating at 80 kV, equipped with a Tracor type TN 2000 energy dispersive microanalyzer. The grids, placed in a low-background holder, were tilted at an angle of 24° towards the detector. The axis of the holder was perpendicular to that of the TN 2000. Multiple point analyses were performed for 100 sec lifetime with a spot diameter of 100 nm from a 150 μm condenser II aperture. Beam intensity was controlled between 0.018 and 0.021 μA. In the recorded spectra, peaks were identified with a peak identification program. By introduction of the proper (400 keV wide) regions of interest, net intensities for iron and phosphorus were obtained.

RESULTS

In the six subjects tested, serum ferritin values correlated well with light microscopical gradation of iron deposits (Table 1). In osmium-fixed, unstained ultrathin liver sections of the same patients electron-dense particles of approximately 5 nm could be detected in the parenchymal cell: (a) in clusters and in hepatic lyso-

Received March 4, 1985; accepted August 12, 1985.

[†] Present address: Medical Centre Alkmaar, Wilhelminalaan 12, 1815 JD Alkmaar, The Netherlands.

Address reprint requests to: J. J. M. Marx, M.D., Department of Haematology, University Hospital Utrecht, P. O. Box 16250, 3500 CG Utrecht, The Netherlands.

somes; (b) free in the cytoplasm, and (c) in the lumina of bile canaliculi (Figure 1). These particles were considered to be ferritin on morphological criteria. Also, in the canaliculi, remnants of membranes and other debris were seen. However, among analyzed subjects, the amount of ferritin particles differed considerably (Table 1). In bismuth subnitrate-stained sections of that material, the size of the particles in all localizations was markedly enhanced (Figure 2).

In the cytoplasm bordering the bile canaliculi, coated vesicles were frequently observed and occasionally a coated pit was found between the microvilli bordering

the canalicular lumen (Figure 3). Electron-dense, ferritin containing lysosomal bodies were predominantly located in the cytoplasm around the bile canaliculi (Figure 4). Comparable lysosomal bodies were observed in epithelial cells bordering a bile ductule or bile duct (Figure 5) in one of our patients with grade IV hemochromatosis.

Electron probe microanalysis *in situ* (Figure 1) of particles selected on morphological grounds confirmed the correctness of the criteria by the detection of iron. Ferritin particles both in the cytoplasm and in the canalicular lumina revealed net intensities for iron (Figure 6) with consistent K_{β}/K_{α} ratios. In clusters of particles,

TABLE 1. DIAGNOSIS, BIOCHEMICAL VALUES AND MICROSCOPIC DATA OF SIX TEST SUBJECTS

Biopsy no.	Diagnosis ^a	Patient no.	Serum ferritin ($\mu\text{g/liter}$)	Light microscopy		Electron microscopy	
				Tissue damage	Grade Perl's blue ^b	Amount of ferritin in Cytoplasm	Amount of ferritin in Canaliculi
1	IHC	1	6,000	Fibrosis	IV	++++	++++
2	IHC	10	6,300	Severe fibrosis	IV	++++	+++
3	SA	3	250	None	II	+++	+/-
4	SA	5	300	None	II	++	++
5 ^c	IHC	1	225	Fibrosis	0	-	+
6 ^d	IHC	10	280	Severe fibrosis	0	-	-

^a IHC, idiopathic hemochromatosis; SA, sideroblastic anaemia.

^b Graded from 0 to IV according to Scheuer et al. (1962).

^c Same patient as no. 1 after phlebotomy treatment.

^d Same patient as no. 2 after phlebotomy treatment.

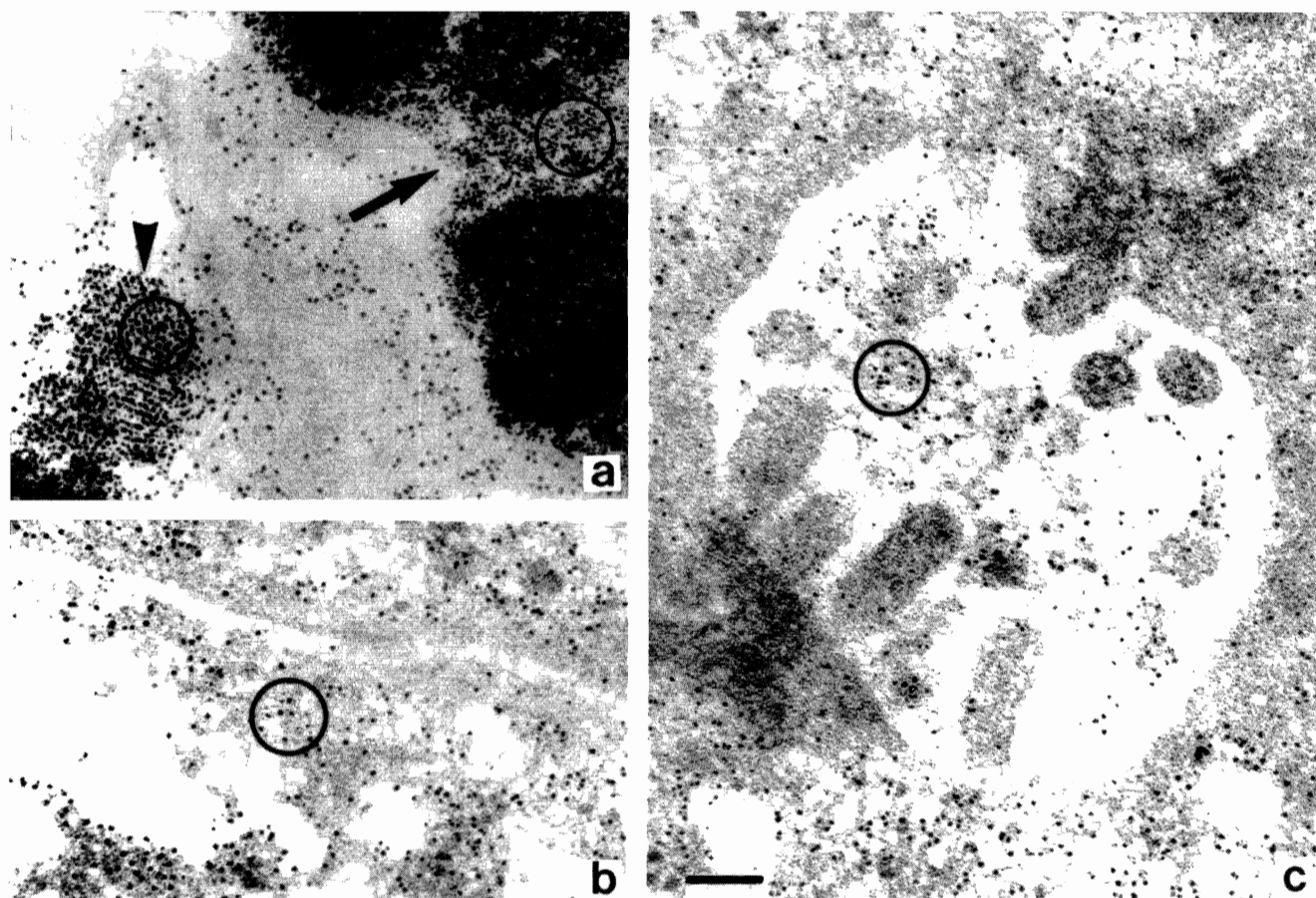


FIG. 1. Tissues not fixed in osmium, unstained section of biopsy 1 (Table 1). Ferritin-like particles; (a) in a cluster (arrowhead) and a lysosomal body (arrow); (b) free in the cytoplasm of the hepatocyte; (c) in the lumen of the bile canalculus. Circle represents spot diameter. 100,000 \times . Bar represents 100 nm.

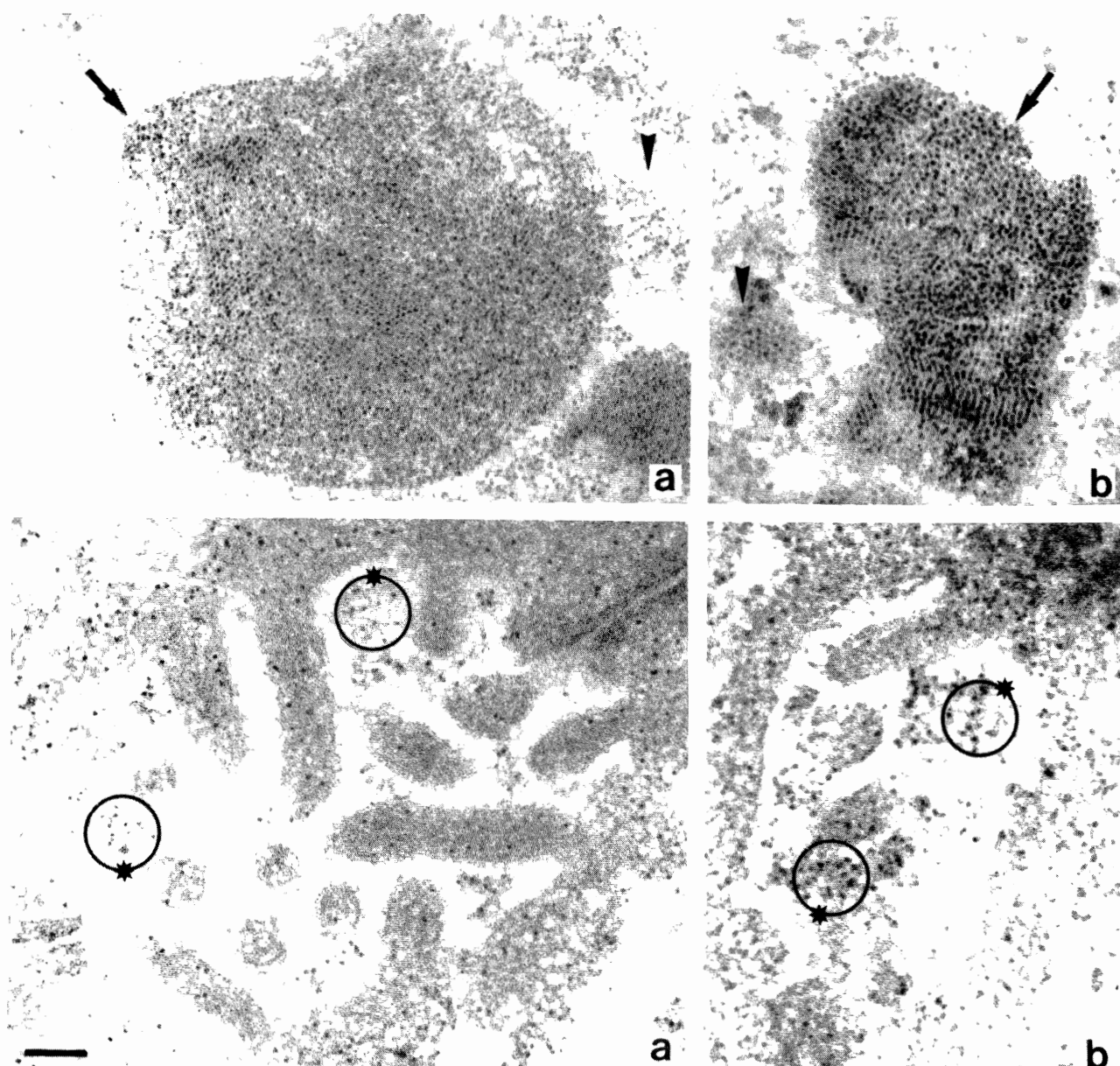


FIG. 2. Tissues not fixed in osmium: (a) unstained, (b) bismuth subnitrate-stained sections of biopsy 1 (Table 1). Ferritin-like particles in a lysosomal body (arrow), free in the cytoplasm of the hepatocyte (arrowhead) and in the lumen of the bile canalculus (asterisk). 92,000 \times . Bar represents 100 nm.

occasionally net intensities for phosphorus could be obtained as well. The mean values of multiple point analyses are presented in Table 2.

DISCUSSION

The morphological observation of 5 nm particles in hepatic cytoplasm and in the lumina of the bile canaliculi, combined with the clear signal obtained by electron probe microanalysis on these particles, indicates that the observed particles contain iron micelles. The phosphorus signal that was obtained suggests the presence of ferric oxyhydroxide crystals associated with phosphorus, as proposed for the ferritin iron core by Michaelis (8). In this way, the occurrence of ferritin was recently demonstrated in various loci in liver, spleen and placenta by Myagkaya and De Bruijn (9) and by De Bruijn and Steyn-Myagkaya (10). Our quantitative data, obtained

by analyzing the particles inside the canaliculi, and those dispersed through the cytoplasm were comparable. However, it should be emphasized that within a defined spot area (100 nm), a variable amount of particles may be present. Moreover, the core of the ferritin particles present in the analyzed volume may contain different amounts of iron atoms (11) which can explain the high standard deviations of the mean data of our observations.

Bismuth subnitrate definitely enhanced the size of the ferritin particles in cytoplasm, lysosomes and canalicular lumina, suggesting the presence of stainable protein around the iron micelle (7). It is of interest that lysosomal ferritin appears to have a stainable protein coat, as lysosomal degradation of ferritin protein is a well-established fact. Hoy and Jacobs (12) presented data indicating that, in lysosomes, polymerization of ferritin protein may occur, and recently Richter (13) proposed a scheme

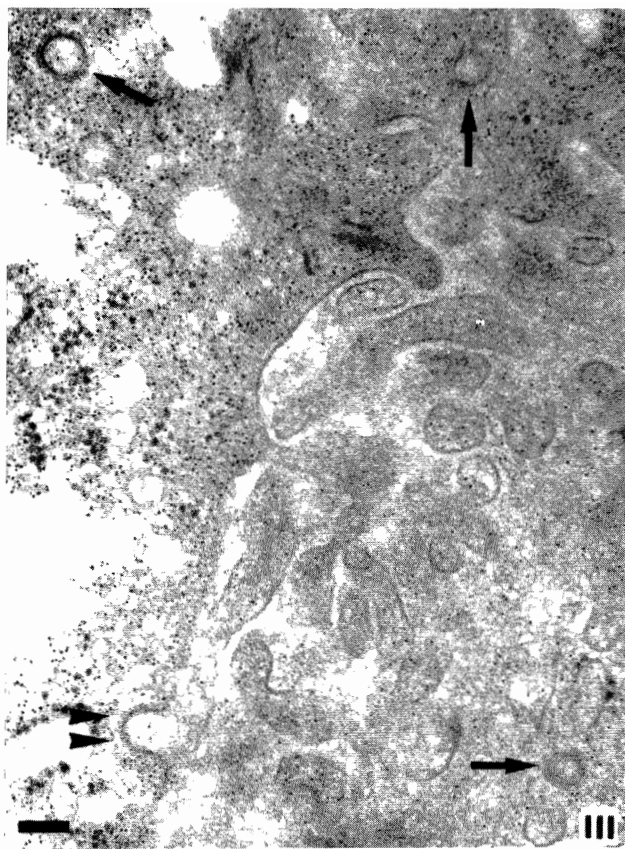


FIG. 3. (Left) Tissues fixed in osmium, stained section of biopsy 2 (Table 1). Coated pit (arrowheads) within and coated vesicles (arrows) near the plasma membrane bordering the bile canalculus. 62,000 \times . Bar represents 100 nm.

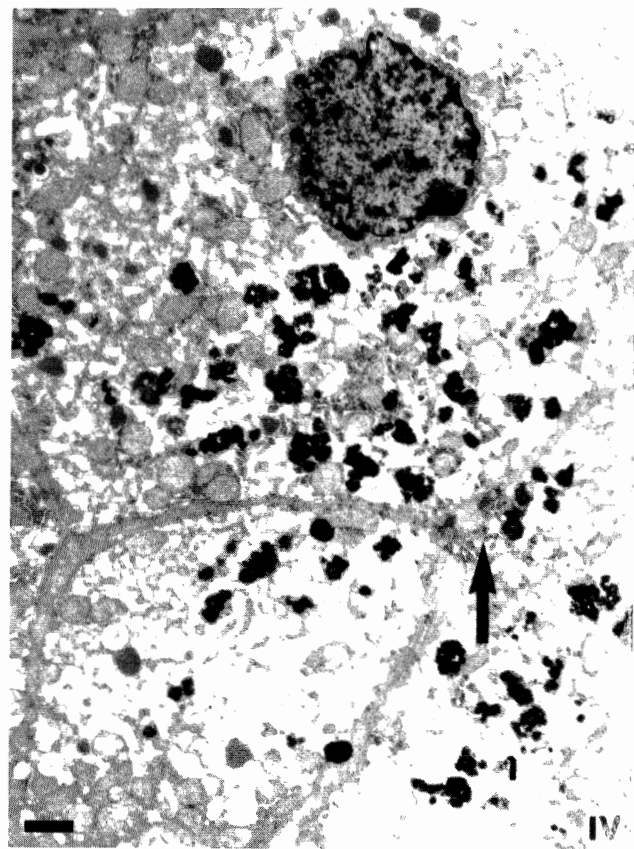


FIG. 4. (Right) Tissues fixed in osmium, stained section of biopsy 2 (Table 1). Peribiliary (arrow) localization of the iron-containing lysosomal bodies. 6,000 \times . Bar represents 1 μ m.

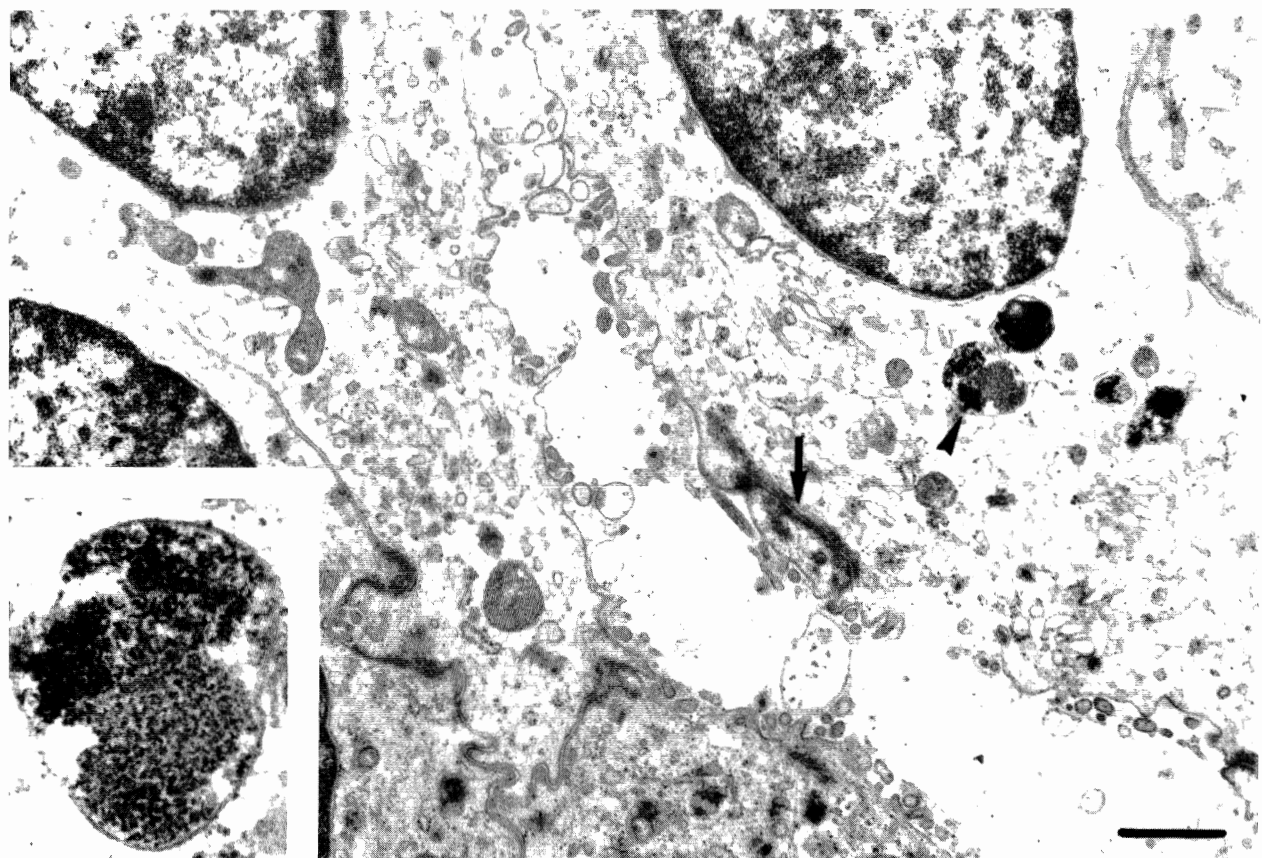


FIG. 5. Tissues fixed in osmium, stained section of biopsy 1 (Table 1). Epithelial cell bordering bile ductule or duct with electron-dense lysosomal bodies. 14,000 \times . (Arrow) Desmosome. (Arrowhead) See inset: higher magnification of ferritin-containing lysosomal body. Bar represents 1 μ m.

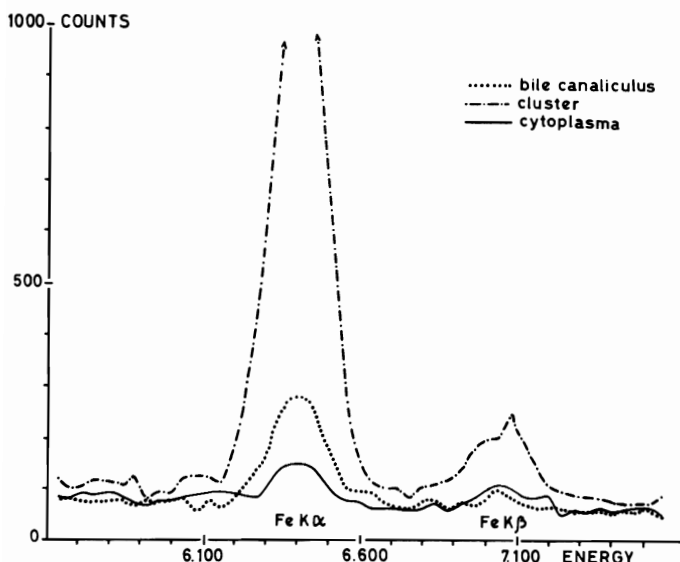


FIG. 6. Iron spectra of three point analyses *in situ* (spot 100 nm). X axis: energy of X-ray emission in KeV. Y axis: intensities in counts per 100 sec lifetime.

TABLE 2. ELECTRON PROBE MICROANALYSIS *IN SITU*^a

Element	Particles in clusters (n = 21)	Particles in cytoplasm (n = 26)	Particles in canaliculi (n = 20)
FeK α	3,172 ± 496	337 ± 120	325 ± 150
FeK β	369 ± 57	59 ± 60	55 ± 29
PK α	216 ± 100	* ^b	* ^b
FeK β /FeK α	0.116	0.156	0.169

^a Mean net intensities for iron (K α and K β) and phosphorus (K α) of n point analyses in counts per 100 sec lifetime; spot size 100 nm.

^b Only two values for phosphorus obtained.

in which decomposition of ferritin protein is preceded by denaturation accompanied by loss of solubility. Our observation of bismuth subnitrate staining of lysosomal as well as free ferritin particles in the cytoplasm and bile canaliculi indicates that the metallic bismuth adheres to the protein mantle regardless of the conformational state of the protein. Thus, the stainable ferritin particles observed in the canalicular lumina are either (FeOOH)_x cores surrounded by holoferitin, which are comparable to free cytoplasmic ferritin particles, or (FeOOH)_x cores surrounded by denatured or polymerized protein, comparable to their lysosomal counterparts.

It is very unlikely that localization of ferritin particles inside the lumina of the bile canaliculi is an artifact associated with displacement of ferritin during sectioning because comparable particles could only be observed inside lysosomal bodies, and not in other cell organelles such as smooth and rough endoplasmic reticulum and mitochondria. We assume, therefore, that the observed intraluminal electron-dense iron-containing particles are indeed excreted ferritin.

Our observations are in agreement with other published data. In an ultrastructural and biochemical study on iron-loaded rats, Bradford et al. (14) have demonstrated ferritin particles and remnants of secondary lysosomes within the canalicular lumina, which were interpreted as excretion of iron and lysosomal contents.

Preliminary data of a biochemical study on bile of iron-loaded rats (Cleton, M. I. et al., *Proc. Dutch Fed. Meeting 1983; 24:77*, Abstract) indicated a concomitant rise of total liver iron and ferritin protein in the bile.

In man, localization of stainable iron deposits predominantly around the bile canaliculi is well known from light microscopical observations (3), and stainable iron deposits can be seen in the epithelial cells of the bile duct in more severe cases of iron overload. In the present study, ferritin-containing lysosomes were observed in severe overload in cells bordering a bile ductulus or duct, indicating an involvement of the biliary system in iron excretion. However, in the canalicular lumen, ferritin particles were found in subjects with different grades of hemosiderosis, regardless of the cause of iron overload and the degree of fibrosis. This indicates that biliary excretion of ferritin may be a vital part of the mechanism of iron excretion by the hepatic parenchymal cells. In this context, it is very interesting that, in the lamprey, bile ducts and canaliculi degenerate and ultimately disappear during metamorphosis. This disappearance is associated with the accumulation of high concentrations of iron in cytoplasmic-dense bodies of hepatocytes (15). This observation also is highly suggestive for a function of the biliary system in hepatic iron excretion.

On the mechanism of iron excretion into the bile, three main theories can be found in the literature: (a) the excretion of iron takes place by transmembrane movement of ferritin particles (16, 17); (b) secondary lysosomes fuse with the cell membrane, and their contents are subsequently excreted into the bile (14), and (c) Fe⁺⁺⁺ is converted to Fe⁺⁺ before it passes the cell membrane (18).

With respect to our morphological observations, we can only speculate on the transport mechanism of ferritin into the bile. Lysosomal "defecation" into the bile has been reported (14, 19, 20). The observed coated pits in and coated vesicles around the biliary plasma membrane may contain recaptured membrane material (21, 22) after extrusion of lysosomal contents, including ferritin. However, there is a faint indication of ferritin particles inside the lumen of one of the coated pits, so these vesicles may as well be indicative for a direct shuttle of, among other things, ferritin particles from the blood (via receptor mediated endocytosis) into the bile.

In summary, we conclude, based upon: (1) a clear signal for iron obtained by electron probe microanalysis *in situ* and (2) the enhancement of size of the particles *in situ* by staining with bismuth subnitrate, that the particles observed in the canalicular lumina are indeed ferritin. We assume that, in man, the biliary system is involved in the excretion of ferritin via the liver parenchymal cell.

REFERENCES

- Clegg CA, Fitton JE, Harrison PM, et al. Ferritin: molecular structure and iron-storage mechanisms. *Prog Biophys Molec Biol* 1980; 36:56-86.
- Richter GW. The iron-loaded cell—the cytopathology of iron storage. A review. *Am J Pathol* 1978; 91:363-396.
- Scheuer PJ. Liver biopsy interpretation, 2nd ed. London: Ballière, Tindall and Cassell, 1977.
- Zuyderhoudt FMJ, Vos P, Jörning GGA, et al. Ferritin in liver plasma and bile of the iron-loaded rat. In: Urushizaki I, Aisen P,

- Listowsky I, et al., eds. Structure and function of iron storage and transport proteins. Amsterdam: Elsevier, 1983: 215–216.
5. Scheuer PJ, Williams R, Muir AR. Hepatic pathology in relatives of patients with haemochromatosis. *J Pathol Bacterial* 1962; 84:53–64.
 6. Van Oost BA, van den Beld B, Cloin LGLM, et al. Measurement of ferritin in serum: application in diagnostic use. *Clin Biochem* 1984; 17:263–270.
 7. Ainsworth SK, Karnovsky MJ. An ultrastructural staining method for enhancing the size and electron opacity of ferritin in thin sections. *J Histochem Cytochem* 1972; 20:225–229.
 8. Michaelis L. Ferritin and apoferitin. *Adv Prot Chem* 1947; 3:53–66.
 9. Myagkaya GL, De Bruijn WC. X-ray microanalysis of cellular localization of ferritin in mammalian spleen and liver. *Micron* 1982; 13:7–21.
 10. De Bruijn WC, Steyn-Myagkaya GL. *In situ* X-ray microanalysis of ferritin. *Beitr Electronenmikroskop Direktabb Oberfl* 1981; 14:423–426.
 11. Treffry A, Harrison PM. Incorporation and release of inorganic phosphate in horse spleen ferritin. *Biochem J* 1978; 171:313–320.
 12. Hoy TG, Jacobs A. Ferritin polymers and the formation of haemosiderin. *Br J Haematol* 1974; 49:593–602.
 13. Richter GW. Studies of iron overload. *Lab Invest* 1984; 50:26–33.
 14. Bradford WD, Elchlepp JG, Arstila AU, et al. Iron metabolism and cell membranes. I. Relation between ferritin and haemosiderin in bile and biliary excretion of lysosome contents. *Am J Pathol* 1969; 56:201–228.
 15. Youson JH, Sargent PA, Sidon EW. Iron loading in the livers of metamorphosing lampreys, *Petromyzon marinus* L. *Cell Tissue Res* 1983; 234:109–124.
 16. Iancu IC, Neustein HB, Landing BH. The liver in thalassemia major: ultrastructural observations. In: Porter R, Fitzsimons DW, eds. Iron metabolism, Ciba Foundation Symposium 51. Amsterdam: Elsevier, 1977: 293–316.
 17. Parmley RT, May EM, Spicer SS, et al. Ultrastructural distribution of inorganic iron in normal and iron-loaded hepatic cells. *Lab Invest* 1981; 44:475–485.
 18. De Duve C, Wattiaux R. Functions of lysosomes. *Ann Rev Physiol* 1966; 28:435–441.
 19. Kerr JFR. Liver cell defaecation: an electron microscope study of the discharge of lysosomal residual bodies in the cellular space. *J Pathol* 1970; 100:99–103.
 20. Kramer MF, Geuze JJ. Redundant cell-membrane regulation in the exocrine pancreas after pilocarpine stimulation of secretion. In: Ceccarelli B, Clementi F, Meldolesi J, eds. International symposium on cell biology and cytopharmacology. New York: Raven Press, 1974: 87–97.
 21. Douglas WW, Nagasawa J, Schulz R. Electron microscopic studies on the mechanism of posterior pituitary hormones and the significance of microvesicles ("synaptic vesicles"): evidence of secretion by exocytosis and formation of microvesicles as byproduct of this process. In: Heller H, Lederis R, eds. Subcellular organization and function in endocrine tissues. Cambridge, England: University Press, 1971: 353–378.
 22. Heuser JE, Reese TS. Evidence for recycling of synaptic vesicle membrane during transmitter release at frog neuromuscular junctions. *J Cell Biol* 1973; 57:315–344.